Linker Region of a Halobacterial Transducer Protein Interacts Directly with Its Sensor Retinal Protein†

Yuki Sudo,‡,§ Hideyasu Okuda,§ Masaki Yamabi,‡ Yuta Fukuzaki,§ Masaki Mishima,§ Naoki Kamo,‡ and Chojiro Kojima*,§

Laboratory of Biophysical Chemistry, Graduate School of Pharmaceutical Sciences, Hokkaido University, Sapporo 060-0812, Japan, and Laboratory of Biophysics, Graduate School of Biological Sciences, Nara Institute of Science and Technology, 8916-5 Takayama, Ikoma, Nara 630-0192, Japan

Received November 18, 2004; Revised Manuscript Received January 25, 2005

ABSTRACT: *p*HtrII, a *pharaonis* halobacterial transducer protein, possesses two transmembrane helices and forms a signaling complex with *pharaonis* phoborhodopsin (*p*pR, also called *pharaonis* sensory rhodopsin II, NpSRII) within the halobacterial membrane. This complex transmits a light signal to the sensory system located in the cytoplasm. It has been suggested that the linker region connecting the transmembrane region and the methylation region of *p*HtrII is important for binding to *p*pR and subsequent photosignal transduction. In this study, we present evidence to suggest that the linker region itself interacts directly with *p*pR in addition to the interaction in the membrane region. An *in vitro* pull-down assay revealed that the linker region bound to *p*pR, and its dissociation constant (K_D) was estimated to be approximately 10 μM using isothermal titration calorimetry (ITC). Solution NMR analyses showed that *p*pR interacted with the linker region of *p*HtrII (*p*HtrII$^{G83-Q149}$) and resulted in the broadening of many peaks, indicating structural changes within this region. These results suggest that the *p*HtrII linker region interacts directly with *p*pR. There was no demonstrable interaction between the C-terminal region of *p*pR (*p*pR$^{Gly224-His247}$) and either the linker region (*p*HtrII$^{G83-Q149}$) or the transmembrane region (*p*HtrII$^{M1-E114}$) of *p*HtrII. On the basis of the NMR, CD, and photochemical data, we discuss the structural changes and role of the linker region of *p*HtrII in relation to photosignal transduction.

The *pharaonis* halobacterial transducer protein, *p*HtrII, from *Natronomonas (Natronobacterium) pharaonis* (*1*), is a two-transmembrane helical protein and belongs to a family of two-transmembrane helical methyl-accepting chemotaxis proteins (MCPs) (*2*−*4*). MCPs exist as homodimers composed of a ∼50−60-kDa subunit and form the ternary complex with CheA and CheW. Chemical stimuli activate phosphorylation cascades that modulate flagella motors (*5*). In relation to chemoreception in bacteria, MCPs act not only as transducers but also as signal receptors. In terms of photoreception in *Natronomonas pharaonis*, a direct interaction is required between *p*HtrII and the photosignal receptor *pharaonis* phoborhodopsin (*p*pR,[1] also called *pharaonis* sensory rhodopsin II, NpsRII) (*1*, *6*). *p*pR transmits light signals to *p*HtrII through changes resulting from the interaction, and *p*HtrII eventually activates phosphorylation cascades that modulate flagella motors. The active (signaling) intermediates of the *p*pR/*p*HtrII complex are referred to as the M and O intermediates (*7*). Using these sensing systems, *N. pharaonis* avoids harmful near-UV light (λ < 520 nm).

*p*pR is a member of the seven-transmembrane helical retinal group of proteins (*8*) that includes rhodopsin (*9*), bacteriorhodopsin (*10*), and others (*11*, *12*). *p*pR and *p*HtrII are stable within the membrane and *n*-dodecyl-β-D-maltoside micelles (*13*, *14*). Expression systems utilizing *Escherichia coli* cells can provide large amounts of *p*pR and *p*HtrII proteins (several mg/L culture) (*15*). Consequently, *p*pR and *p*HtrII have been well-characterized over the past few years using various methods (for reviews, see refs *1*, *8*, *16*, and *17*). Sudo et al. demonstrated a 2:2 stoichiometry in the *p*pR/*p*HtrII complex (*18*) and calculated the binding constant between *p*pR and *p*HtrII under various conditions (*19*, *20*). Figure 1 shows the crystal structure of the *p*pR/*p*HtrII complex (*21*). Of particular importance is the hydrogen-bonding network between Tyr199^{ppR} and Asn74^{pHtrII} and between Thr189^{ppR} and Glu43^{pHtrII}/Ser62^{pHtrII} and the phenolic ring of Tyr199^{ppR} and Phe28^{pHtrII} (*14*, *22*). Furthermore, the importance of Thr189^{ppR}, Asp193^{ppR}, and Thr204^{ppR} for the interaction has also been examined (Yamabi et al., manuscript in preparation).

*p*HtrII is composed of four regions consisting of two-transmembrane segments (TM1 and TM2), a linker region, a methylation region, and a signaling domain. Kim et al. reported on the X-ray structure of the methylation region and the signaling region of a serine chemotaxis receptor (Tsr)

† This work was supported by grants from Japanese Ministry of Education, Culture, Sports, Science, and Technology.

* To whom correspondence should be addressed. Telephone: 81-743-72-5571. Fax: 81-743-72-5579. E-mail: kojima@bs.naist.jp.

‡ Hokkaido University.

§ Nara Institute of Science and Technology.

[1] Abbreviations: *p*pR, *pharaonis* phoborhodopsin; *p*HtrII, *pharaonis* halobacterial transducer II; DM, *n*-dodecyl-β-D-maltoside; OG, *n*-octyl-β-D-glucoside; NMR, nuclear magnetic resonance; ITC, isothermal titration calorimetry; K_D, dissociation constant; GST, glutathione-*S*-transferase; CD, circular dichroism; HSQC, heteronuclear single-quantum correlation; TM, transmembrane segment; *p*HtrII$^{G83-Q149}$, *p*HtrII fragment from Gly83 to Gln149.

10.1021/bi047573z CCC: $30.25
Published on Web 03/26/2005

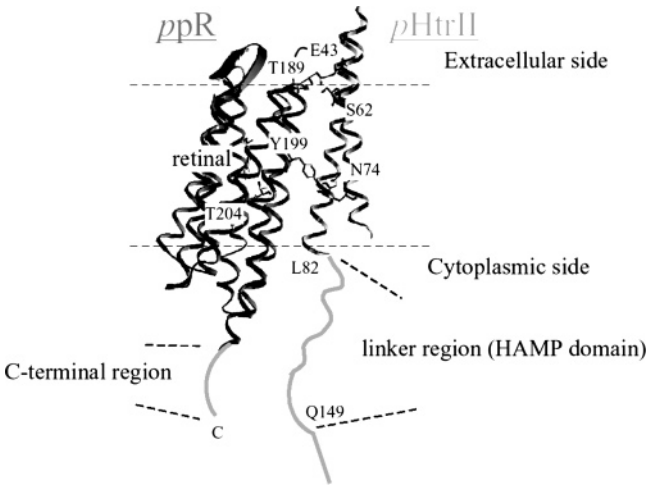

FIGURE 1: X-ray crystallographic structure of the *p*pR/*p*HtrII complex. The structure was obtained from the Protein Data Bank (PDB code 1H2S). *p*pR and *p*HtrII form the signaling complex in the dark and photolyzed state. Light stimulation activates *p*pR and triggers trans−cis photoisomerization of the retinal chromophore. Relaxation of the retinal leads to the functional processes during the photocycle. *p*pR transmits light signals to *p*HtrII in the membrane. *p*HtrII forms a ternary complex with CheA and CheW and activates phosphorylation cascades that modulate flagella motors. In this paper, the *p*HtrII linker region and the C-terminal region of *p*pR were designated as the regions from *p*HtrII^{Leu83} to *p*HtrII^{Gln149} and from *p*pR^{Gly224} to *p*pR^{His247}, respectively. The membrane normal is roughly in the vertical plane of this figure, and the top and bottom regions correspond to the extracellular and cytoplasmic sides, respectively.

(*23*). The X-ray structure of the transmembrane region of *p*HtrII in the *p*pR/*p*HtrII complex has recently been reported (*21*) (Figure 1). Tsr belongs to the two-transmembrane helical MCPs (*2*, *24*). Although these results have facilitated the next stage of research to do with photosignal transduction, detailed structural investigations concerning the linker region connecting the membrane region and the methylation region of MCPs have not been reported. The linker region posesses what is referred to as a HAMP domain, which is typically found in various proteins such as histidine kinases, adenylyl cyclases, methyl-accepting chemotaxis/phototaxis proteins, and phosphatases (*2*, *24*). This domain plays crucial roles in the phosphorylation or methylation of homodimeric receptors by transmitting conformational changes from the periplasmic to the cytoplasmic domain. It has been suggested that the linker region of the transducer may participate in the interaction with the sensor retinal pigment because certain residues within the linker region of HtrI (the *Halobacterium salinarum* transducer protein) modulate the sensory rhodopsin (sR, also called sensory rhodopsin I, sRI) photocycle (*4*, *25*). Umemura et al. reported that the sensing of cytoplasmic pH by chemoreceptors involves the linker region (*26*). Recently, Yang et al. reported that the E−F loop of *p*pR was located near the part of the *p*HtrII linker region based on probe accessibility data, disulfide formation assays, the flash photolysis analysis, as well as the FRET analysis (*27*). In this paper, we demonstrate that the linker region of *p*HtrII (*p*HtrII$^{G83-Q149}$) interacts directly with *p*pR.

MATERIALS AND METHODS

Protein Expression and Purification. The *p*pRHis (His refers to a hexa-histidine tag at the C terminus) expression plasmid was constructed as previously described (*28*). The GST-*p*HtrII$^{G83-Q149}$ gene was prepared by employing a PCR methodology. Primer 5′-GGATCCTGGGCGGTGACAC-CGCCGCCTCGCTTTC-3′ (the underlined bases indicate the added restriction site for *Bam*HI) and the reverse primer 5′-TTATGTGCCTGCTCTGCGTCCTCGCGAGCGTTC-3′ (the underlined bases indicate the added stop codon) were designed for the PCR. The PCR product was subcloned into the pGEM-T Easy (Promega) plasmid vector. The *Bam*HI and *Eco*RI digested fragment was ligated to a pGEX5X-3 vector (Amarsham). This cloning strategy resulted in the following N- and C-terminal peptide sequence: GST-*p*HtrII^{83}GGDTA- - -AEQAQ^{149}.

*p*pR was expressed in *E. coli* strain BL21 (DE3) (Invitrogen, Carlsbad, CA) at 37 °C in 2× YT medium containing ampicillin and subsequently induced by the addition of 1 mM IPTG and 10 μM all-*trans* retinal. Preparation of crude membranes and purification of *p*pR was performed as previously described (*29*). GST-*p*HtrII$^{G83-Q149}$ and GST only were overexpressed in *E. coli* strain BL21 (DE3) star cells (Invitrogen, Carlsbad, CA) and subsequently induced by the addition of 1 mM IPTG (Wako Pure Chemical Industries, Osaka, Japan). *p*pR proteins possessing a histidine tag at the C terminus were solubilized with 1.0% *n*-dodecyl-β-D-maltoside (DM) and subsequently purified using a Ni column as previously described (*29*).

IPTG-induced cells that expressed GST alone and GST-*p*HtrII linker were harvested by centrifugation at 4 °C. Pellets were resuspended in buffer A [50 mM Tris-HCl (pH 8.0) and 5 mM $MgCl_2$] and then broken by sonication. The supernatants were collected by ultracentrifugation (140000*g* for 30 min at 4 °C) to remove the membrane fraction. GST and GST-*p*HtrII$^{83-149}$ were then applied to a glutathione sepharose 4B resin column. The resin was washed extensively with buffer B [50 mM Tris-HCl (pH 8.0) and 300 mM NaCl] to remove nonspecifically bound proteins. GST and GST-tagged *p*HtrII were then eluted with buffer C [50 mM Tris-HCl (pH 8.0), 300 mM NaCl, and 10 mM glutathione]. The sample medium was exchanged by Amicon Ultra (Millipore, Bedford, MA) filtration and the samples were finally suspended in a buffer solution containing 150 mM NaCl, 50 mM Tris-HCl (pH 7.5), and 1 mM $CaCl_2$. Purified GST-*p*HtrII$^{83-149}$ was incubated with Factor Xa (0.5 unit/mg of protein) for ∼3−4 h at 4 °C. The reaction was stopped by the addition of a protease inhibitor (1,5-dansyl-Glu-Gly-Arg-chloromethyl ketone dihydrochloride, Calbiochem). GST-digested *p*HtrII$^{G83-Q149}$ was separated by gel-filtration chromatography in a buffer solution containing 150 mM NaCl, 50 mM Tris-HCl (pH 7.5), and 1 mM $CaCl_2$. A final yield of 30 mg of *p*HtrII$^{83-149}$/L of cell culture was obtained.

Uniformly ^{15}N-single-labeled and ^{15}N-,^{13}C-double-labeled proteins for NMR experiments were prepared by growing the cells in standard minimal medium containing 0.5 g/L ^{15}N-ammonium chloride (Isotec Inc., Miamisburg, OH) or ^{15}N-ammonium chloride and 1.0 g/L ^{13}C-D-glucose (Isotec Inc., Miamisburg, OH). Transformed cells were initially grown at 37 °C in 1 mL of LB medium and were inoculated directly into 200 mL of isotope-labeled standard minimal M9 medium followed by inoculation in 4 L of labeled medium.

Binding Assay between the pHtrII Linker Region (pHtrII$^{G83-Q149}$) and ppR. GST-tagged *p*HtrII$^{G83-Q149}$, GST-digested *p*HtrII$^{G83-Q149}$, and *p*pR were concentrated by Amicon Ultra (Millipore, Bedford, MA) filtration. Buffer solutions were exchanged completely by dialysis against a buffer solution [300 mM NaCl, 10 mM Tris-HCl (pH 8.0), and 1% OG] for 1 week using a 3-kDa cutoff dialysis cassette (Molecular cut off, 3000, Daiichi Pure Chemicals Co. Ltd. Tokyo, Japan). The protein concentration of *p*pR and *p*HtrII was determined using the molar extinction coefficient at 500 nm (40 000 M^{-1} cm^{-1}) (*30*) and 280 nm (Tyr (1420 M^{-1} cm^{-1}), respectively.

An *in vitro* pull-down assay was performed using a glutathione sepharose column essentially as previously described (*18*, *31*). Purified *p*HtrII$^{G83-Q149}$ (300 μM) and *p*pR (30 μM) were mixed in a molar ratio of 1:10 in buffer B containing 1% OG and then incubated for 1 h at room temperature with gentle stirring. After the mixed samples were bound to the glutathione sepharose resin, the resin was poured into a chromatography column and washed extensively with buffer B (about 5-fold volume against the column volume) to remove nonspecifically bound proteins. Bound *p*pR was eluted with buffer C.

For the isothermal titration calorimetry (ITC) experiments, the *p*pR and *p*HtrII$^{G83-Q149}$ sample buffer solutions were exchanged completely by dialysis against a buffer solution [150 mM NaCl, 10 mM Tris-HCl (pH 8.0), and 0.05% DM] for 1 week using a 3-kDa cutoff dialysis cassette. The protein concentration of *p*pR and *p*HtrII was 0.35 and 0.03 mM, respectively. All ITC experiments were performed at 308 K on a VP-ITC Micro Calorimeter (Microcal Inc). For control experiments, DM-containing buffers were used to ensure that there was no effect because of the detergent. The binding parameters were estimated using the following binding scheme:

$$p\text{pR}/p\text{HtrII}_n \leftrightarrow p\text{pR} + np\text{HtrII}$$

where *n* represents the number of *p*HtrII molecules required for the formation of a complex with *p*pR. Data were evaluated by employing the Origin-ITC software package.

Flash Photolysis with or without pHtrII$^{G83-Q149}$. The apparatus and procedure for flash spectroscopy was essentially as previously described (*32*). The decay rate of the M photointermediate of the wild-type *p*pR (20 μM) with or without *p*HtrII$^{G83-Q149}$ (80 μM) and *p*HtrII$^{M1-L159}$ (80 μM) was observed at 350 nm. Truncated *p*HtrII expressed from position 1−159 was used instead of the whole protein because the truncated transducer tightly interacts with *p*pR [K_D = 0.1 μM (in the dark state)] (*22*). The temperature was maintained at 20 °C.

NMR Spectroscopy. NMR experiments for $^{13}C/^{15}N$-labeled *p*HtrII$^{G83-Q149}$ were performed at 283 K on a Bruker Avance 500 spectrometer with a ^{1}H [$^{13}C/^{15}N$] pulse field gradient cryogenic probe in a buffer solution containing 50 mM KCl and 50 mM KP_i (pH 6.5) without detergent. NMR experiments for $^{13}C/^{15}N$-labeled *p*pR were performed at 303 K on a Bruker Avance 500 spectrometer in a buffer solution containing 50 mM KCl, 10 mM citric acid (pH 5.0), and 3% 1,2-dihexanoyl-*sn*-glycero-3-phosphocholine (DHPC) as a detergent. The protein concentration was 1.8 and 0.4 mM for *p*HtrII and *p*pR, respectively. The assignments of the ^{1}H, ^{13}C, and ^{15}N resonances of *p*HtrII$^{G83-Q149}$ and *p*pR were obtained using ^{1}H-^{15}N HSQC and a series of triple-resonance experiments: HN(CO)CACB, HNCACB, HNCO, HN(CA)-CO, and (H)N(CO-TOCSY)NH incorporating pulsed field gradients, water flip-back pulses, and a sensitivity enhancement scheme. All data were processed using NMRPipe (*33*) and analyzed using Sparky (http://www.cgl.ucsf.edu/home/sparky/) (*34*). The NMR experiments for $^{13}C/^{15}N$-labeled *p*HtrII$^{G83-Q149}$ in the presence of *n*-octyl-β-D-glucoside (OG) were performed at 283 K on a Bruker Avance 500 MHz spectrometer in a buffer solution containg 50 mM KCl and 50 mM KP_i (pH 6.5).

CD Spectroscopy. The CD spectrum was recorded on a JASCO (Tokyo, Japan) J-720W CD spectropolarimeter. The CD spectrum was recorded between 260 and 200 nm (0.1 cm cell) at 0.1 nm intervals with a scan speed of 20 nm/min. Signals were averaged over 6 separate scans. The protein concentration was 20 μM in a buffer solution containing 50 mM KP_i, 50 mM KCl, and OG (free, 0.5, 1.0, and 7.2%).

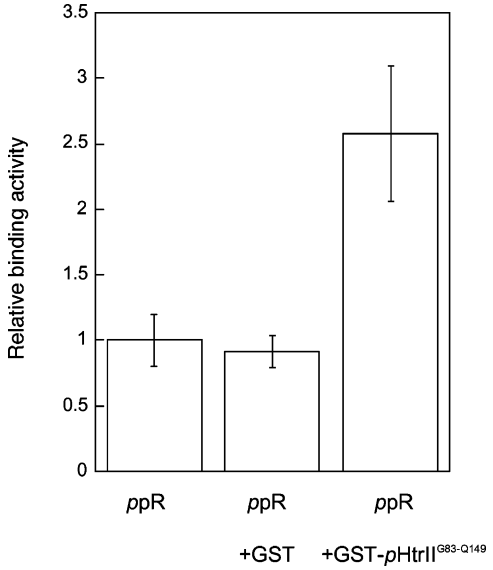

FIGURE 2: *In vitro* pull-down assay using glutathione sepharose resin. *p*pR was applied to the column without GST and GST-*p*HtrII$^{G83-Q149}$ (lane 1), with GST (lane 2), and with GST-*p*HtrII$^{G83-Q149}$ (lane 3). After the column was washed extensively with buffer B (for details, see the Materials and Methods) to remove nonspecifically bound proteins, bound proteins were eluted with buffer C (see the Materials and Methods). The eluted material was collected, and the UV−vis spectrum of *p*pR (λ_{max} = 500) was then measured.

RESULTS

Direct Interaction between the pHtrII Linker Region and ppR. In an effort to determine whether the *p*HtrII linker region (*p*HtrII$^{G83-Q149}$) interacts with *p*pR, we performed the *in vitro* pull-down assay (see the Materials and Methods and refs *18* and *31*). *p*pR adsorbed onto the glutathione sepharose 4B resin containing immobilized GST-*p*HtrII$^{G83-Q149}$. Figure 2 shows the adsorbed fraction of *p*pR in the presence of GST (lane 2) and in the absence or presence of GST-*p*HtrII$^{G83-Q149}$ (lanes 1 and 3, respectively). Specifically adsorbed *p*pR was detected in the presence of GST-*p*HtrII$^{G83-Q149}$.

The interaction between the *p*HtrII linker region (*p*HtrII$^{G83-Q149}$) and *p*pR was then quantitatively examined

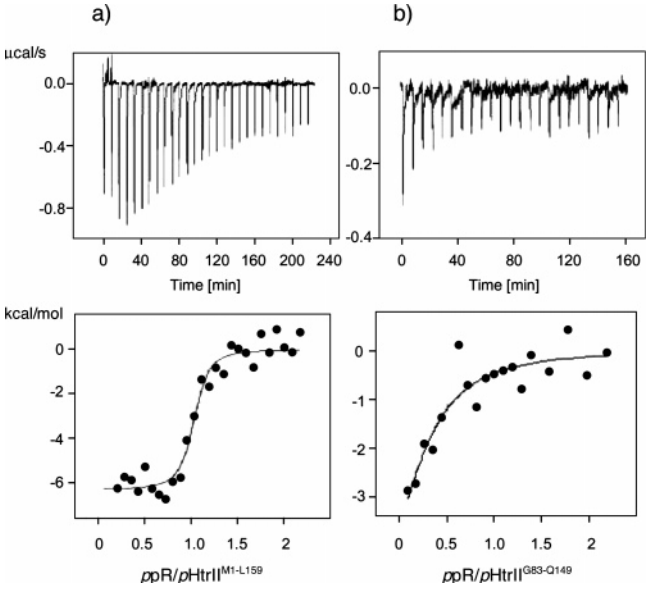

FIGURE 3: Isothermal calorimetric titration curves of *p*pR titrated with *p*HtrII$^{M1-L159}$ (a) and *p*HtrII$^{G83-Q149}$ (b). The upper panels represent the raw data. The lower panels represent the enthalpy changes per mole plotted as a function of the molar ratio of *p*pR to *p*HtrII. The solid lines represent best-fit curves (for details, see the Materials and Methods). The dilution heat of *p*pR is subtracted in these calculations. The binding parameters determined are listed in Table 1.

using ITC. Figure 3 shows the titration curves of *p*pR with *p*HtrII$^{M1-L159}$ and *p*HtrII$^{G83-Q149}$. Our ITC experiments were performed under the conditions established by Engelhard and co-workers (*22*). In these experiments, *p*HtrII$^{M1-L159}$ and *p*HtrII$^{G83-Q149}$ were maintained at 318 and 308 K, respectively, and *p*pR was added in increments of 10 μL using a syringe. The dissociation constant of *p*HtrII$^{M1-L159}$ (0.10 μM) was similar to the previously reported value (0.16 μM) (*22*). The dissociation constant (K_D) of *p*HtrII$^{G83-Q149}$ (10 μM) increased by nearly two orders and was almost identical to that of the signaling complex (*p*pR$_M$/*p*HtrII) (15 μM), as determined by flash photolysis (*18*). Our ITC results and those of other researchers are summarized in Table 1.

Table 1: Dissociation Constants (K_D) of Various *p*pR/*p*HtrII Mutant Complexes for the Ground State of *p*pR as Determined by ITC

	temperature (K)	pH	K_D (μM)	reference
*p*HtrII$^{M1-T157}$	318	8	0.16	*a*
*p*HtrII$^{M1-E114}$	318	8	0.23	*a*
*p*HtrII$^{M1-L159}$	318	8	0.1	this paper
*p*HtrII$^{G83-Q149}$	308	8	10	this paper
*p*HtrII$^{M1-L159}$ (interaction with *p*pR$_M$)	293	7.2	15	*b*

[a] Data from Hippler-Mreyen et al. (*22*). [b] Data from Sudo et al. (*18*).

From these binding assays, we concluded that the *p*HtrII linker region (*p*HtrII$^{G83-Q149}$) was able to interact directly with *p*pR in the dark state. Thus, the transmembrane and linker regions of *p*HtrII are both important in facilitating a direct and tight interaction with *p*pR.

Detailed Analysis of the Interaction between the pHtrII Linker Region and ppR by Solution NMR Spectroscopy. Solution NMR spectroscopy was performed in an effort to analyze the details of the *p*HtrII$^{G83-Q149}$–*p*pR interaction. Figure 4 shows a ^{1}H-^{15}N HSQC NMR spectrum of 1.8 mM *p*HtrII$^{G83-Q149}$ in 50 mM KP$_i$ (pH 6.5) and 50 mM KCl at

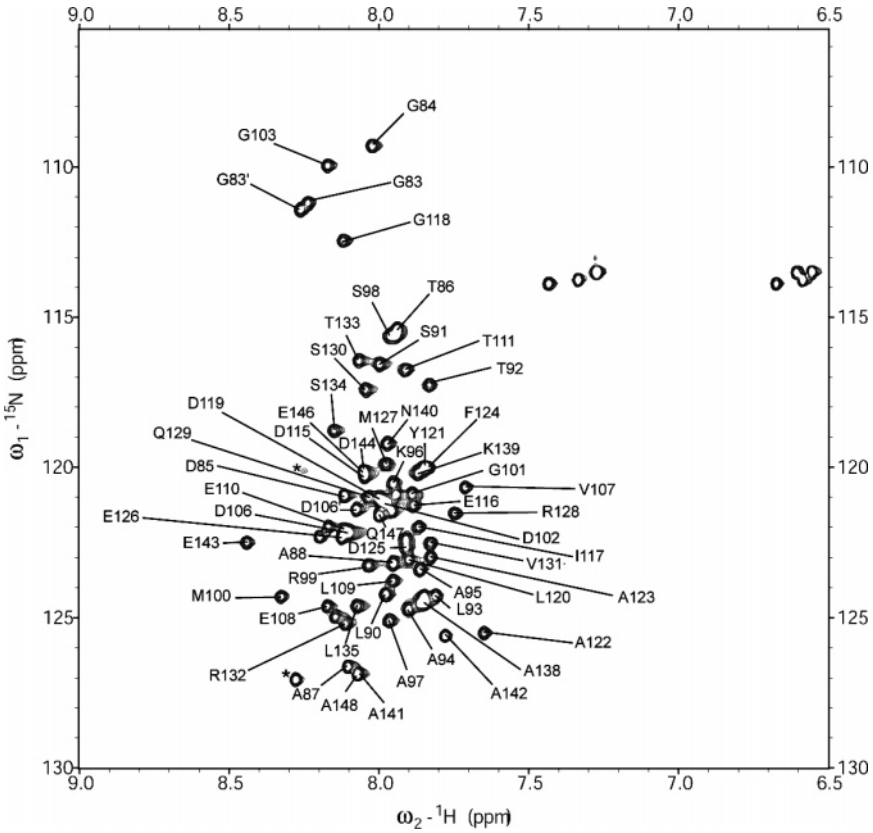

FIGURE 4: Two-dimensional ^{1}H-^{15}N HSQC spectrum of *p*HtrII$^{G83-Q149}$. The spectrum was recorded in 50 mM KCl and 50 mM KP$_i$ (pH 6.5) at 283 K on a 500 MHz NMR spectrometer. The assignments of the backbone amide protons are labeled.

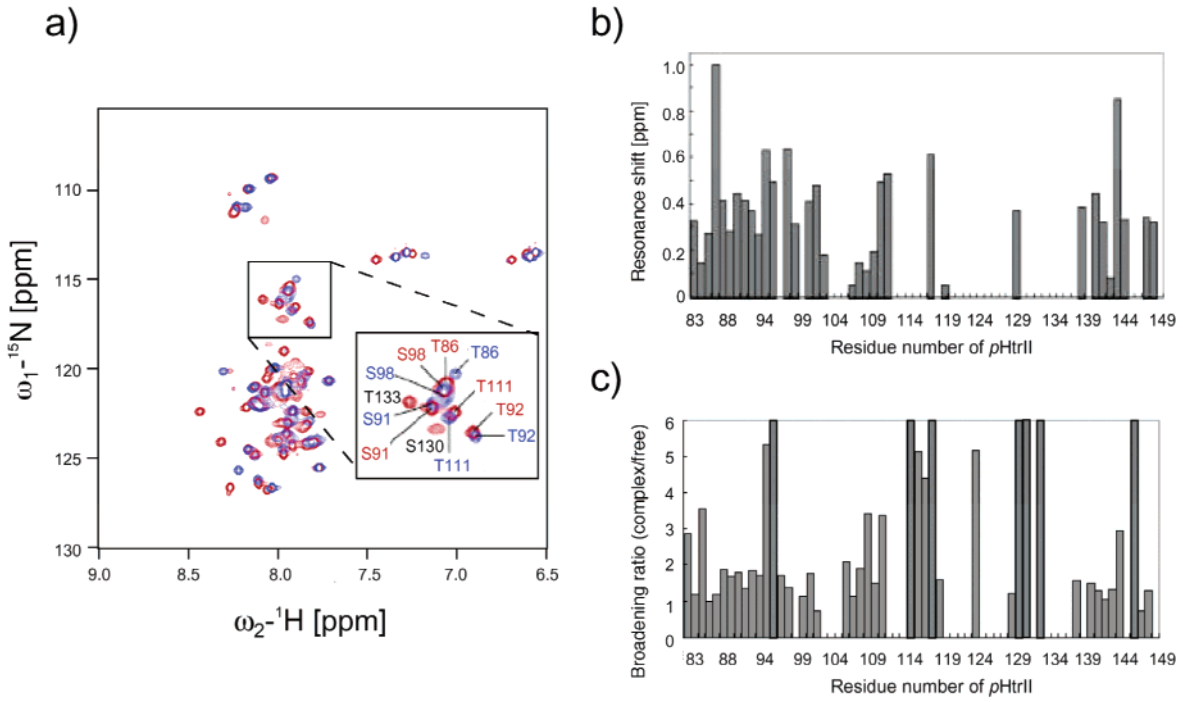

FIGURE 5: (a) Two-dimensional ^{1}H-^{15}N HSQC spectra of *p*HtrII$^{G83-Q149}$ with (blue) or without (red) *p*pR. Both spectra were recorded in 50 mM KP_i (pH 6.5) and 50 mM KCl at 283 K with 1% OG. (b and c) *p*pR-induced chemical-shift changes and the broadening ratios (complex/free ^{1}H line width), respectively, of the amide cross-peaks of *p*HtrII$^{G83-Q149}$.

283 K without detergent. Almost all of the signals from the backbone amide groups were observed. Backbone ^{1}H, ^{13}C, and ^{15}N resonances of 60 residues were assigned using conventional triple-resonance techniques, resulting in identification of the random structure based on ^{13}C chemical shifts. The assigned resonances are labeled in the figure. The ^{1}H-^{15}N HSQC spectra of 0.25 mM *p*HtrII$^{G83-Q149}$ in 50 mM KP_i (pH 6.5) and 50 mM KCl at 283 K with 1% OG as a detergent in the absence or presence of *p*pR (0.25 mM) are shown in Figure 5a as red and blue, respectively. *p*pR-induced resonance shifts and broadening were detected for many peakes, indicating that *p*HtrII$^{G83-Q149}$ interacts with *p*pR. This result is consistent with results of the aforementioned binding assays (Figures 2 and 3). Parts b and c of Figure 5 show the amino acid residues of *p*HtrII$^{G83-Q149}$ that showed resonance shifts and broadening, respectively, induced following association with *p*pR. The broadening of the resonance peaks originated from the middle part of the linker region (*p*HtrII$^{E114-R132}$), indicating that some structural changes in this region may occur.

Effect of the C-Terminal Region of ppR on the Interaction with the pHtrII Linker Region. The interaction between *p*pR and the *p*HtrII linker region (*p*HtrII$^{G83-Q149}$) was examined using stable isotope-labeled *p*pR (not *p*HtrII). Figure 6a shows a ^{1}H-^{15}N two-dimensional NMR spectrum of 0.4 mM *p*pR in 10 mM citric acid (pH 5.0) and 50 mM KCl at 303 K. Backbone ^{1}H, ^{13}C, and ^{15}N resonances of 23 residues in the C-terminal region of *p*pR (Figure 6b) were assigned using a conventional triple-resonance procedure. The assigned resonances are labeled in the figure. The ^{1}H-^{15}N HSQC spectra of 0.20 and 0.3 mM *p*pR in the absence or presence of 0.20 mM *p*HtrII$^{G83-Q149}$ and 0.3 mM of *p*HtrII$^{M1-E114}$ are shown in parts d and c of Figure 6, respectively. *p*HtrII-induced resonance shifts and broadening were not detected. Thus, the C-terminal region of *p*pR (*p*pR$^{Gly224-His247}$) does not participate in the interaction with *p*HtrII within the detergent micelles.

Does pHtrII Linker Region Interact with the M Photointermediate of ppR? Sudo et al. estimated the K_D value of the complex between the M intermediate of *p*pR (*p*pR$_M$) and *p*HtrII$^{M1-L159}$ (*18*). In an effort to determine whether this linker region (*p*HtrII$^{G83-Q149}$) can interact with *p*pR$_M$, a photochemical assay (see the Materials and Methods and refs *19* and *20*) was employed. Figure 7 shows the decay of the M photointermediate of *p*pR in the presence or absence of *p*HtrII. The decays of *p*pR$_M$ with or without *p*HtrII$^{M1-L159}$ are shown as gray lines, reproduced from ref *18*, and that of *p*pR$_M$ with *p*HtrII$^{G83-Q149}$ is shown as black dots. The molecular ratios of both *p*pR/*p*HtrII$^{M1-L159}$ and *p*HtrII$^{G83-Q149}$ were 1:10. The decay rate constant of the M photointermediate of *p*pR in the absence or presence of *p*HtrII$^{M1-L159}$, as well as that in the presence of *p*HtrII$^{G83-Q149}$, was 1.66, 0.82, and 1.69 s^{-1}, respectively. No significant change in the M decay rate was observed when *p*HtrII$^{83-149}$ was added to a molar ratio of *p*pR/*p*HtrII$^{G83-Q149}$ = 1:30 (data not shown). When *p*pR interacts with *p*HtrII$^{M1-L159}$, the decay rate of the M photointermediate of *p*pR changes ~2−4-fold. Thus, *p*HtrII$^{G83-Q149}$ does not interact with *p*pR$_M$, although the fragment might still physically interact but possibly not sufficiently to alter the decay rate.

DISCUSSION

Hippler-Mreyen et al. reported that the dissociation constant of *p*HtrII$^{M1-T157}$ (0.16 μM) was nearly 3 orders smaller than the value of *p*HtrII^{M1-L82} (>100 μM) (*22*). *p*HtrII^{M1-L82} lacks the linker region of *p*HtrII. They concluded that *p*HtrII$^{G83-T157}$ is important for the interaction with *p*pR. Yang et al. made use of the fluorescence resonance energy

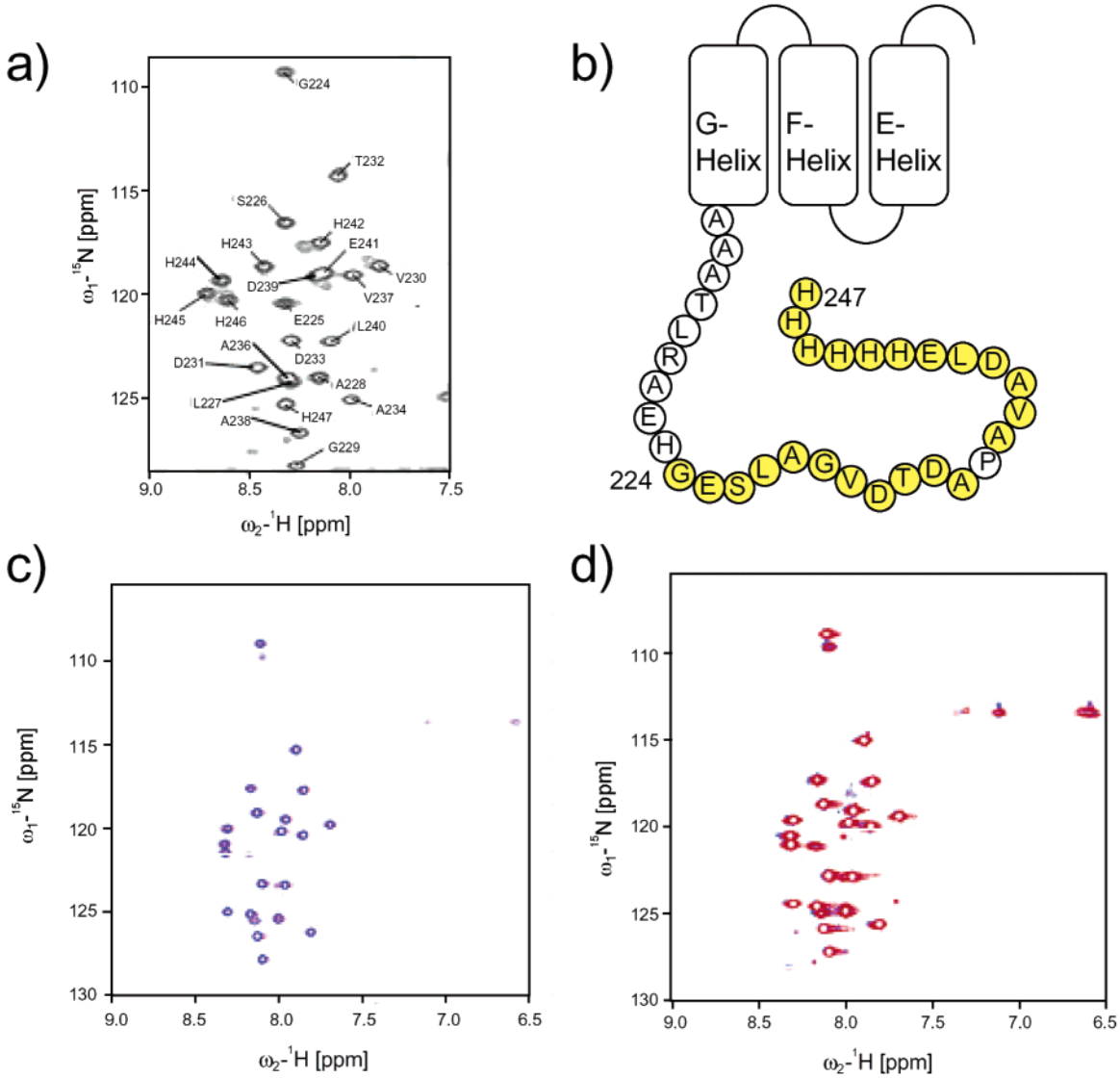

FIGURE 6: (a) Two-dimensional ^{1}H-^{15}N HSQC spectrum of *p*pR. The spectrum was recorded in 50 mM KCl and 50 mM KP_i (pH 6.5) at 283 K on a 500 MHz NMR spectrometer. The assignments of the backbone amide protons are labeled. (b) 23 residues located in the C-terminal region of *p*pR that were assigned. (c and d) ^{1}H-^{15}N HSQC spectra of the ^{15}N-labeled *p*pR in the absence (red) or presence (blue) of *p*HtrII$^{G83-Q149}$ (c) and *p*HtrII$^{M1-E114}$ (d).

transfer (FRET) method and concluded that the interaction site of *p*pR with the linker region is located near Ser-154 (*27*). From mutation analyses, Spudich and co-workers reported that *p*HtrII^{Gly83} and *p*HtrII^{Ala88} are important residues involved in photosignal transduction (*35*). In this paper, we demonstrated that the *p*HtrII linker region interacted directly with *p*pR. Our results are consistent with their data. Thus, the *p*HtrII linker region is important in facilitating a direct interaction with *p*pR that eventually results in phototransduction by the *p*pR/*p*HtrII complex.

OG was used as a detergent in the solution NMR analyses because *p*pR was not stable in the detergent-free solution. However, OG may affect the structure of the *p*HtrII linker region. From the CD spectroscopic measurements, it was determined that the secondary structure of the linker region changed from a random to an α-helical structure following the addition of OG. The cmc of the detergent (about 1%) is critical in determining the formation of the α helix (Figure 8a). This result is consistent with NMR experiments where the addition of OG altered the ^{1}H-^{15}N HSQC spectra in a manner dependent on the micelle concentration of OG (Figure 8b). Additionally, the resonance shifts and broadening were mainly detected in two short regions, the N-terminal and C-terminal parts of the *p*HtrII linker region, suggesting the formation of two α helices. These results suggest that the linker region would act as the chameleon sequence. Formation of an α helix is consistent with the data presented by Danielson et al., where the linker region of Tar corresponding to the *p*HtrII linker region forms an α helix by the cysteine and disulfide bond scanning method (*36*).

The nature of the OG-induced resonance shifts and broadening related to the *p*HtrII linker region was clearly different from those of the *p*pR-induced spectral changes (see Figures 5 and 8). These results reflect the presence of a specific interaction between the *p*HtrII linker region and *p*pR and that the observations made were not derived from detergent-induced changes. *p*pR-induced chemical-shift changes of the *p*HtrII signals mainly occurred in the N-terminal part of the *p*HtrII linker region spanning about 20 residues, suggesting that this N-terminal region possesses specific binding sites for *p*pR.

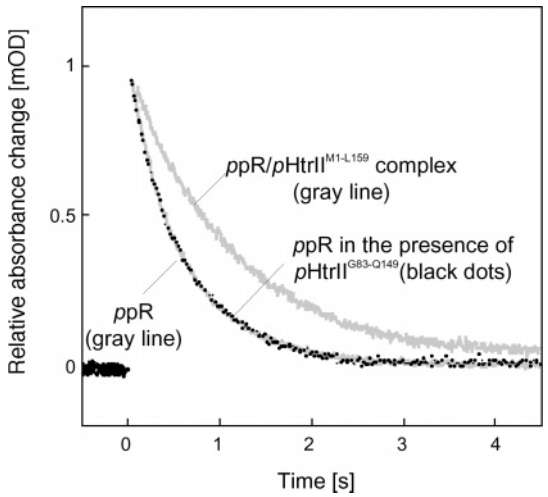

FIGURE 7: Decay of the M photointermeditate of *p*pR with or without *p*HtrII$^{G83-Q149}$ and *p*HtrII$^{M1-L159}$. The decay was monitored at 350 nm. Samples were suspended in a buffer solution containing 400 mM NaCl, 10 mM Tris-HCl (pH 7.0), and 1% *n*-dodecyl-*β*-D-maltoside (DM). The temperature was maintained at 20 °C. The decay curves of *p*pR$_M$ with or without *p*HtrII$^{M1-L159}$ are represented by gray lines, and that with *p*HtrII$^{G83-Q149}$ is represented by black dots.

From the flash photolysis analysis, it was concluded that *p*HtrII$^{G83-Q149}$ does not interact with *p*pR$_M$ (Figure 7). Signal transduction from *p*pR to *p*HtrII is accompanied by a weakened interaction with *p*pR$_M$ (*14*, *18*, *22*, *31*). Therefore, it seems that the *p*HtrII linker region is perturbed by the M state of *p*pR; that is, the interaction between *p*pR and *p*HtrII becomes weak. Wegener et al. reported that the F helix of *p*pR moves toward *p*HtrII following light activation of *p*pR (*37*). Helix movement during the photocycle in bacteriorhodopsin (BR) has also been reported (*38*, *39*). The helix movement of *p*pR is the signaling trigger to *p*HtrII. Engelhard and co-workers reported that the TM-2 of *p*HtrII rotates by following helix movement of *p*pR (*40*) and have suggested that the switch is in the M1 to M2 reaction (*41*). On the basis of the evidence given in this paper, a new photosignal transduction model is proposed (Figure 9). The movement of the helix in *p*pR and rotation of the TM-2 helix in *p*HtrII occurs. Dissociation and conformational changes in the *p*HtrII linker region, as demonstrated in this paper, follows. Thus, the association/dissociation of the *p*HtrII linker region acts as a signaling switch in this model. Our model is consistent with the paper by Yang et al. (*27*) that the G83F mutant of *p*HtrII, which eliminates the interaction with *p*pR, also eliminates phototaxis signaling.

In conclusion, we show that the *p*HtrII linker region (*p*HtrII$^{G83-Q149}$) interacts directly with *p*pR. Solution NMR analyses in the presence or absence of *p*pR showed that the global structural change of the *p*HtrII linker region occurs because of association with *p*pR. The CD and NMR measurements at various OG concentrations revealed that the *p*HtrII$^{G83-Q149}$ conformational changes are caused by a direct and specific interaction with *p*pR. Flash photolysis analysis showed that *p*HtrII$^{G83-Q149}$ could not interact with *p*pR at the M state. Because the signal transduction from *p*pR to *p*HtrII is accompanied by a weakened interaction with *p*pR$_M$, the dissociation and subsequent conformational changes of the *p*HtrII linker region that follow can effect a transfer of the signal downstream. We propose this scheme as the "linker switch model" for photosignal transduction.

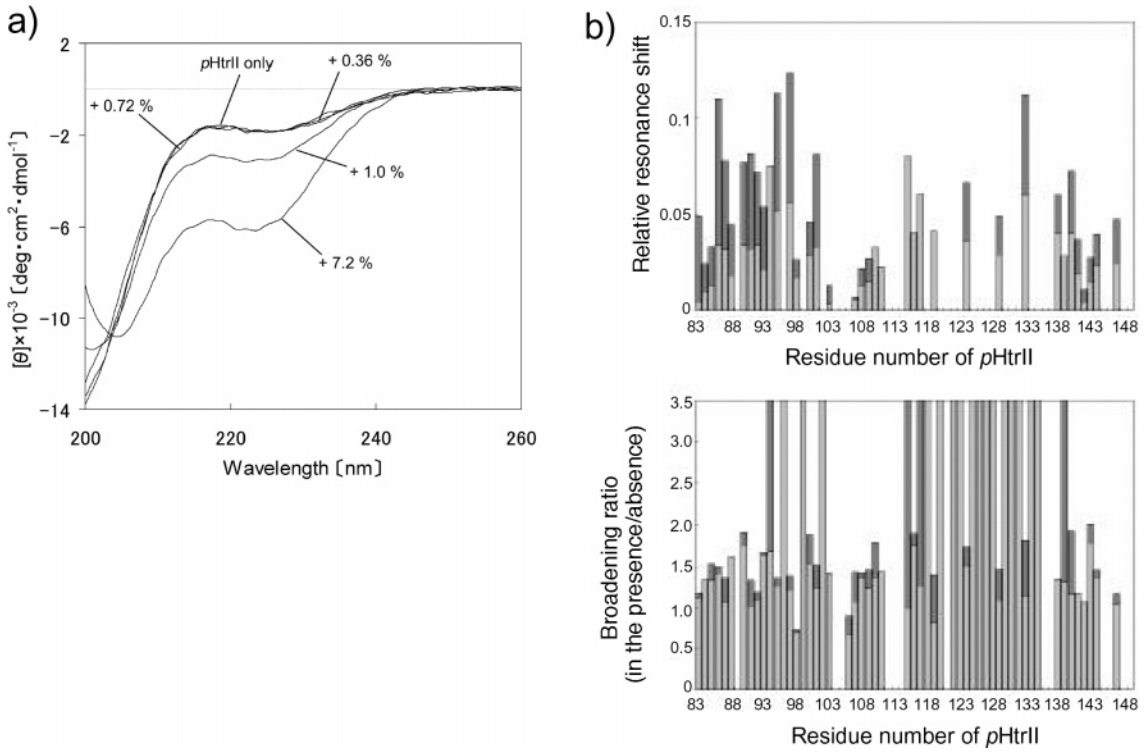

FIGURE 8: (a) CD spectrum of *p*HtrII$^{G83-Q149}$ at various concentrations of OG detergent. The CD spectrum was recorded on a JASCO J-720W CD spectropolarimeter between 200 and 260 nm at 283 K. The spectrum obtained was baseline-corrected. (b) OG-induced chemical-shift changes (top) and the broadening ratios (bottom) (^{1}H line width in the presence/absence of OG) of the ^{1}H-^{15}N HSQC cross-peaks of *p*HtrII$^{G83-Q149}$. Gray bars and black bars in b show the OG-induced changes in the presence of 1.0 and 7.2% OG, respectively.

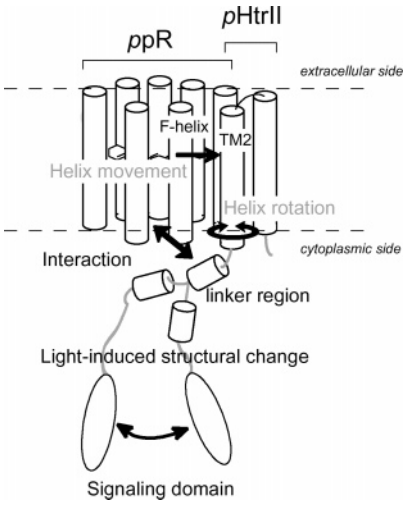

FIGURE 9: Model for photosignal transduction. The photoinduced conformational changes of *p*pR are transmitted to *p*HtrII. Rotation of the F helix of *p*pR induces structural changes in *p*HtrII. Simultaneous dissociation and conformational changes in the linker region then follow. The signal can subsequently be transmitted to CheW and CheA that form a ternary complex with *p*HtrII. Thus, the *p*HtrII linker region can be thought of as a molecular switch for signal transduction.

ACKNOWLEDGMENT

We thank Dr. Harumi Fukada for expert technical assistance in ITC measurement and critical reading of the manuscript and Junko Tsukamoto in N-terminal sequencing and TOF mass spectroscopy. We also thank Toshitatsu Kobayashi for valuable discussions.

REFERENCES

1. Sudo, Y., Kandori, H., and Kamo, N. (2004) Molecular mechanism of protein−protein interaction of *pharaonis* phoborhodopsin/transducer and photosignal transfer reaction by the complex, *Recent Res. Dev. Biophys. 3*, 1−16.
2. Rudolph, J., Nordmann, B., Storch, K. F., Gruenberg, H., Rodewald, K., and Oesterhelt, D. (1996) A family of halobacterial transducer proteins, *FEMS Microbiol. Lett. 139*, 161−168.
3. Falke, J. J., Bass, R. B., Butler, S. L., Chervitz, S. A., and Danielson, M. A. (1997) The two-component signaling pathway of bacterial chemotaxis: A molecular view of signal transduction by receptors, kinases, and adaptation enzymes, *Annu. Rev. Cell Dev. Biol. 13*, 457−512.
4. Hoff, W. D., Jung, K. H., and Spudich, J. L. (1997) Molecular mechanism of photosignaling by archaeal sensory rhodopsins, *Annu. Rev. Biophys. Biomol. Struct. 26*, 223−258.
5. Falke, J. J., and Hazelbauer, G. L. (2001) Transmembrane signaling in bacterial chemoreceptors, *Trends Biochem. Sci. 26*, 257−265.
6. Zhang, X. N., Zhu, J., and Spudich, J. L. (1999) The specificity of interaction of archaeal transducers with their cognate sensory rhodopsins is determined by their transmembrane helices, *Proc. Natl. Acad. Sci. U.S.A. 96*, 857−862.
7. Yan, B., Takahashi, T., Johnson, R., and Spudich, J. L. (1991) Identification of signaling states of a sensory receptor by modulation of lifetimes of stimulus-induced conformations: The case of sensory rhodopsin II, *Biochemistry 30*, 10686−10692.
8. Iwamoto, M., Kandori, H., and Kamo N. (2003) Photochemical properties of *pharaonis* phoborhodopsin (sensory rhodopsin II), *Recent Res. Devel. Chem. 1*, 15−30.
9. Hubbell, W. L., Altenbach, C., Hubbell, C. M., and Khorana, H. G. (2003) Rhodopsin structure, dynamics, and activation: A perspective from crystallography, site-directed spin labeling, sulfhydryl reactivity, and disulfide cross-linking, *Adv. Protein Chem.* 243−290.
10. Lanyi, J. K., and Luecke, H. (2001) Bacteriorhodopsin, *Curr. Opin. Struct. Biol. 11*, 415−419.
11. Bieszke, J. A., Braun, E. L., Bean, L. E., Kang, S., Natvig, D. O., and Borkovich, K. A. (1999) The nop-1 gene of neurospora crassa encodes a seven transmembrane helix retinal-binding protein homologous to archaeal rhodopsins, *Proc. Natl. Acad. Sci. U.S.A. 96*, 8034−8039.
12. Beja, O., Aravind, L., Koonin, E. V., Suzuki, M. T., Hadd, A., Nguyen, L. P., Jovanovich, S. B., Gates, C. M., Feldman, R. A., Spudich, J. L., Spudich, E. N., and DeLong, E. F. (2000) Bacterial rhodopsin: Evidence for a new type of phototrophy in the sea, *Science 289*, 1902−1906.
13. Ikeura, Y., Shimono, K., Iwamoto, M., Sudo, Y., and Kamo, N. (2003) Arg-72 of *pharaonis* phoborhodopsin (sensory rhodopsin II) is important for the maintenance of the protein structure in the solubilized state, *Photochem. Photobiol. 77*, 96−100.
14. Sudo, Y., Yamabi, M., Iwamoto, M., Shimono, K., and Kamo, N. (2003) Interaction of *Natronobacterium pharaonis* phoborhodopsin (sensory rhodopsin II) with its cognate transducer probed by increase in the thermal stability, *Photochem. Photobiol. 78*, 511−516.
15. Shimono, K., Iwamoto, M., Sumi, M., and Kamo, N. (1997) Functional expression of *pharaonis* phoborhodopsin in *Escherichia coli*, *FEBS Lett. 420*, 54−56.
16. Spudich, J. L. (2002) Spotlight on receptor/transducer interaction, *Nat. Struct. Biol. 9*, 797−799.
17. Klare, J. P., Gordeliy, V. I., Labahn, J., Büldt, G., Steinhoff, H. J., and Engelhard, M. (2004) The archaeal sensory rhodopsin II/transducer complex: A model for transmembrane signal transfer, *FEBS Lett. 564*, 219−224.
18. Sudo, Y., Iwamoto, M., Shimono, K., and Kamo, N. (2001) *pharaonis* phoborhodopsin binds to its cognate truncated transducer even in the presence of a detergent with a 1:1 stoichiometry, *Photochem. Photobiol. 74*, 489−494.
19. Sudo, Y., Iwamoto, M., Shimono, K., and Kamo, N. (2002) Tyr-199 and charged residues of *pharaonis* phoborhodopsin are important for the interaction with its transducer, *Biophys. J. 83*, 427−432.
20. Sudo, Y., Iwamoto, M., Shimono, K., and Kamo, N. (2004). Role of charged residues of *pharaonis* phoborhodopsin (seonsory rhodopsin II) in its interaction with the transducer protein, *Biochemistry 43*, 13748−13754.
21. Gordeliy, V. I., Labahn, J., Moukhametzianov, R., Efremov, R., Granzin, J., Schlesinger, R., Buldt, G., Savopol, T., Scheidig, A. J., Klare, J. P., and Engelhard, M. (2002) Molecular basis of transmembrane signalling by sensory rhodopsin II−transducer complex, *Nature 419*, 484−487.
22. Hippler-Mreyen, S., Klare, J. P., Wegener, A. A., Seidel, R., Herrmann, C., Schmies, G., Nagel, G., Bamberg, E., and Engelhard, M. (2003) Probing the sensory rhodopsin II binding domain of its cognate transducer by calorimetry and electrophysiology, *J. Mol. Biol. 330*, 1203−1213.
23. Kim, K. K., Yokota, H., and Kim, S. H. (1999) Four-helical-bundle structure of the cytoplasmic domain of a serine chemotaxis receptor, *Nature 400*, 787−792.
24. Aravind, L., and Ponting, C. P. (1999) The cytoplasmic helical linker domain of receptor histidine kinase and methyl-accepting proteins is common to many prokaryotic signalling proteins, *FEMS Microbiol. Lett. 176*, 111−116.
25. Jung, K. H., and Spudich, J. L. (1996) Protonatable residues at the cytoplasmic end of transmembrane helix-2 in the signal transducer HtrI control photochemistry and function of sensory rhodopsin I, *Proc. Natl. Acad. Sci. U.S.A. 93*, 6557−6561.
26. Umemura, T., Matsumoto, Y., Ohnishi, K., Homma, M., and Kawagishi, I. (2002) Sensing of cytoplasmic pH by bacterial chemoreceptors involves the linker region that connects the membrane-spanning and the signal- modulating helices, *J. Biol. Chem. 277*, 1593−1598.
27. Yang, C. S., Sineshchekov, O., Spudich, E. N., and Spudich, J. L. (2004) The cytoplasmic membrane-proximal domain of the HtrII transducer interacts with E−F loop of photoactivated *Nactronomonas pharaonis* sensory rhodopsin II, *J. Biol. Chem. 279*, 42964−42969
28. Sudo, Y., Furutani, Y., Shimono, K., Kamo, N., and Kandori, H. (2003) Hydrogen bonding alteration of Thr-204 in the complex between *pharaonis* phoborhodopsin and its transducer protein, *Biochemistry 42*, 14166−14172.
29. Kandori, H., Shimono, K., Sudo, Y., Iwamoto, M., Shichida, Y., and Kamo, N. (2001) Structural changes of *pharaonis* phoborhodopsin upon photoisomerization of the retinal chromophore: Infrared spectral comparison with bacteriorhodopsin, *Biochemistry 40*, 9238−9246.

30. Chizhov, I., Schmies, G., Seidel, R., Sydor, J. R., Luttenberg, B., and Engelhard, M. (1998) The photophobic receptor from *Natronobacterium pharaonis*: Temperature and pH dependencies of the photocycle of sensory rhodopsin II, *Biophys. J. 75*, 999−1009.
31. Sudo, Y., Iwamoto, M., Shimono, K., and Kamo, N. (2002) Association between a photointermediate of a M-lacking mutant D75N of *pharaonis* phoborhodopsin and its cognate transducer, *J. Photochem. Photobiol., B 67*, 171−176.
32. Miyazaki, M., Hirayama, J., Hayakawa, M., and Kamo, N. (1992) Flash photolysis study on *pharaonis* phoborhodopsin from a haloalkaliphilic bacterium (*Natronobacterium pharonis*), *Biochim. Biophys. Acta 1140*, 22−29.
33. Delaglio, F., Grzesiek, S., Vuister, G. W., Zhu, G., Pfeifer, J., and Bax, A. (1995) NMRPipe: A multidimensional spectral processing system based on UNIX pipes, *J. Biomol. NMR 6*, 277−293.
34. Goddard, T. D., and Kneller, D. G. *SPARKY 3*, University of California, San Francisco, CA.
35. Yang, C. S., and Spudich, J. L. (2001) Light-induced structural changes occur in the transmembrane helices of the *Natronobacterium pharaonis* HtrII transducer, *Biochemistry 40*, 14207−14214.
36. Danielson, M. A., Bass, R. B., and Falke, J. J. (1997) Cysteine and disulfide scanning reveals a regulatory α-helix in the cytoplasmic domain of the aspartate receptor, *J. Biol. Chem. 272*, 32878−32888.
37. Wegener, A. A., Chizhov, I., Engelhard, M., and Steinhoff, H. J. (2000) Time-resolved detection of transient movement of helix F in spin-labeled *pharaonis* sensory rhodopsin II, *J. Mol. Biol. 301*, 881−891.
38. Vonck, J. (2000) Structure of the bacteriorhodopsin mutant F219L N intermediate revealed by electron crystallography, *EMBO J. 19*, 2152−2160.
39. Radzwill, N., Gerwert, K., and Steinhoff, H. J. (2001) Time-resolved detection of transient movement of helices F and G in doubly spin-labeled bacteriorhodopsin, *Biophys. J. 80*, 2856−2866.
40. Wegener, A. A., Klare, J. P., Engelhard, M., and Steinhoff, H. J. (2001) Structural insights into the early steps of receptor-transducer signal transfer in archaeal phototaxis, *EMBO J. 20*, 5312−5319.
41. Rivas, L., Hippler-Mreyen, S., Engelhard, M., and Hildebrandt, P. (2003) Electric-field dependent decays of two spectroscopically different M-states of photosensory rhodopsin II from *Natronobacterium pharaonis*, *Biophys. J. 84*, 3864−3873.

BI047573Z